View metadata, citation and similar papers at core.ac.uk
brought to you by CORE
provided by Defence Science Journal

Defence Science Journal, Vol. 57, No. 3, May 2007, pp. 261-269
© 2007, DESIDOC

Optimising Performance of a Cantilever-type Micro Accelerometer Sensor

B.P. Joshi[1], A.S. Chaware[2], and S.A. Gangal[2]

[1]*Armament Research and Development Establishment, Pune-411 021*
[2]*University of Pune, Pune-411 007*

ABSTRACT

A technique for optimising performance of cantilever-type micro acceleration sensor has been developed. Performance of a sensor is judged mainly by its sensitivity and bandwidth. Maximising product of these two important parameters of inertial sensors helps to optimise the sensor performance. It is observed that placement of a lumped mass (add-mass) on the sensor's proof-mass helps to control both sensitivity and the first resonant frequency of the cantilever structure to the designer's choice. Simulation and modelling of various dimensions of rectangular structures for acceleration sensor with this novel add-mass technique are discussed. Coventorware MEMSCAD has been used to model, simulate, and carry out FEM analysis. A simple analytical model is discussed to elaborate the mechanics of cantilever-type micro accelerometer. The comparison of the results obtained from analytical model and the finite element simulations reveal these to be in good agreement. The advantages of this technique for choosing the two most important sensor parameters (i.e., sensitivity and bandwidth) of an inertial sensor are brought out.

Keywords: Micro sensor, accelerometer, piezoresistive sensor, add-masstechnique, FEA, MEMSCAD

NOMENCLATURE

C	Distance from fixed-end at which force F is acting
E	Modulus of elasticity
f	Ratio of distance of CG of structure from fixed-end to beam length
F	Force
I_z	Moment of inertia of about Z-axis flexure
K	Proportionality constant
k	Flexure stiffness constant
L_b	Length of flexure beam
M	Bending moment for a force acting at any location X from the fixed-end
M_{pm}	Mass of proof-mass
S	Sensitivity
t	Thickness of the flexure
v	Deflection
X	Location from the fixed-end
ω	Resonant frequency

1. INTRODUCTION

Microelectromechanical sensors (MEMS)-based acceleration sensors are mostly either capacitive or piezoresistive-type. A piezoresistive- type acceleration (inertial) sensor basically consists of a proof-mass attached to a micro-cantilever (flexure) made out of silicon[1-8]. The flexure gets deflected when the

Revised 19 November 2006

sensor is subjected to inertial force. This deflection causes the development of strain in the flexure, which can be measured by implanted piezoresistor bridge on surface of *Si*. It is usually desired to make accelerometer as sensitive as possible while maintaining its higher bandwidth, i.e., higher first resonant frequency. Roylance and Angel[9] have established that both these requirements contradict each other, i.e., when it was tried to maximise the sensitivity, the bandwidth was reduced and vice versa. Therefore, the challenge lies in getting maximum performance out of the sensor by maximising the product of the two parameters of primary interest, i.e., sensitivity and resonant frequency[10].

A design optimisation procedure discussed by Seidel and Csepregi[11] was for maximising one of the parameters at a time while specifying the other one[11]. A methodology was given to select the geometrical parameters of the structure such as width, length and thickness of flexure. Lim[12], *et al*. have presented a novel bridge structure which results in increase in sensitivity of nearly two orders of magnitude higher than the common cantilever–beam designs.

The present study concentrates on cantilever-type of structure since it is still popular owing to its simple design and usefulness in applications such as sensing missile acceleration. One way to increase the sensitivity is by increasing the mass of the proof-mass[11]. However, this drastically reduces the resonant frequency of the sensor. To overcome this problem, a novel technique has been devised where a small lumped mass (termed as add-mass) of heavier material is placed on the proof-mass. Position of this add-mass decides the location of centre of gravity (CG) of the structure, which in turn determines the structure's resonant frequency and sensitivity. When add-mass is placed nearer to the fixed-end on the proof-mass, the resonant frequency is higher and stress (i.e., in turn sensor sensitivity) is lower. Whereas, when the add-mass is moved away from the fixed-end, the resonant frequency gradually reduces and the stress in flexure increases[13]. The structure with an add-mass is shown in Fig. 1. The structure consisting of flexure and proof-mass can be easily fabricated using standard bulk micro-machining techniques and the deposition of lumped mass on the proof-mass may be carried out using either casting or LIGA technique[14].

Finite element model (FEM) simulations were carried out using Coventorware MEMSCAD software to analyse the dynamic behaviour of the structure for prediction of stress developed in the flexure and structure's first resonant frequency. The behaviour of the structure in respect of bandwidth and sensitivity corresponding to the position of the add-mass and method of optimising sensor parameters are discussed.

2. MEMSCAD MODELLING

Coventorware 2003 is a design tool with large number of modules, right from 2-D mask design, solid modelling, static and dynamic loading, and Finite element analysis of MEMS devices. This

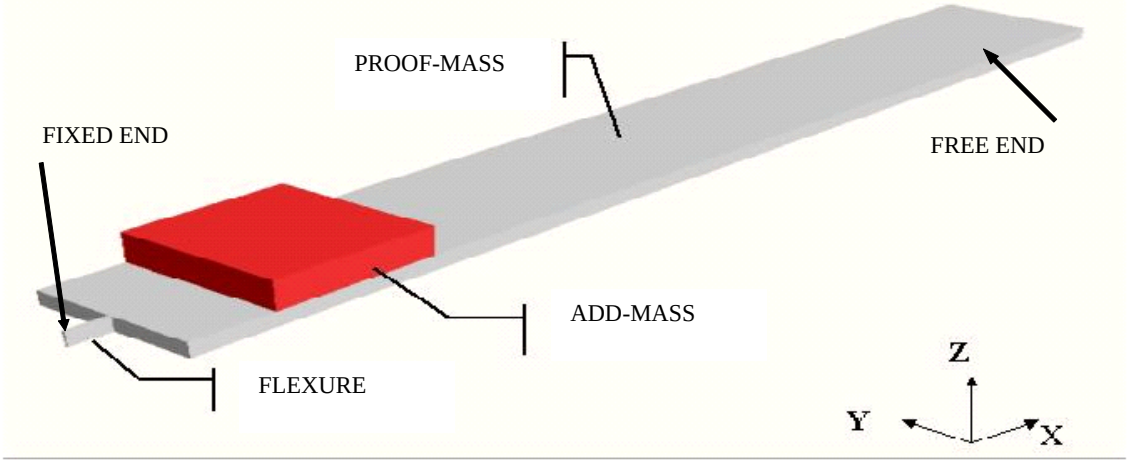

Figure 1. Schematic of cantilever-type acceleration sensor with add-mass.

tool was used for the creation of acceleration sensor structure, which consists of a small cantilever termed as flexure. A proof-mass is attached to this flexure (Fig. 1). The flexure is a spring element, which gets deflected on application of inertial force. The deflection of the flexure generates stress in this element. The amount of deflection, and therefore the stress developed, depends on many factors such as mass of the proof-mass, CG of the structure, material density, flexure dimensions, proof-mass dimensions, etc. The modelling starts with the design of 2-D layout of the structure. Masks for each part of the inertial sensor, i.e., flexure, proof-mass, add-mass and planar deposit are created in layout editor. These parts have dimensions in x-y plane as given below.

Flexure: 100 μm × 8 μm

Proof-mass: 3000 μm × 400 μm

Add-mass: 400 μm × 400 μm

Although it is possible to create complicated shapes in CAD, the shape of sensor structure was chosen to be of simple rectangular geometry for proving the concept and for a comparison with the analytical solution from empirical formulas. The add-mass width was taken the same as that of the proof-mass because its effect on the shift in CG in such cases is found to be most effective. Although real-life sensors would have much smaller sized proof-mass, larger dimensions of proof-mass were chosen only from the simulation point of view to obtain amplified results. The next step was to create a fabrication process file, which is akin to steps involved in idealised fabrication process of the device structure. A process editor was used to create a recipe for 3-D model building by defining various parameters such as substrate, deposition of selected material, etching-type, depth and masks to be used. A structure with thickness of 50 μm, 50 μm, and 100 μm, respectively for flexure, proof-mass and add-mass were created. This solid model was then meshed for further finite element analysis. (Fig. 2).

Only the flexure was fine-meshed because strain concentration was to be studied at flexure. The model was subjected to various types of solvers in the CAD tool after defining proper boundary conditions and applied forces in the solver setup. Mechanical analysis was run to obtain stress values developed in flexure after applying inertial force in Y-axis. The von-Mises theory was used to pick up maximum stress generated in the flexure. The stress value thus obtained can be regarded as sensitivity of the device. Modal analysis was run on the model to find first resonant frequency of

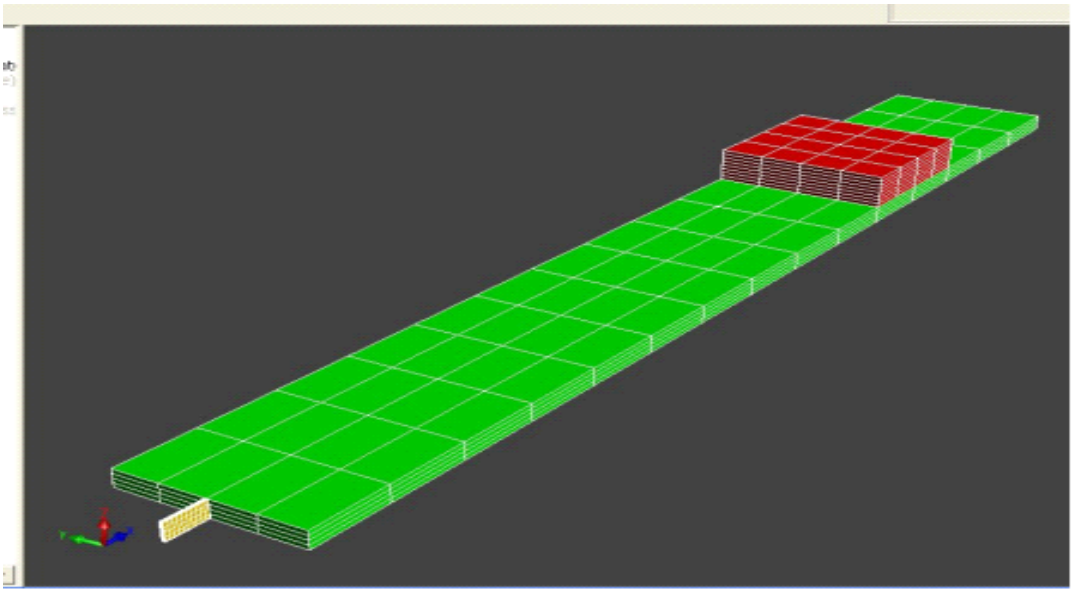

Figure 2. 3–D Mesh model of acceleration sensor modelled in Coventorware MEMSCAD.

the structure, which is regarded as the bandwidth of the device[9].

The sensitivity and resonant frequency (bandwidth) of a cantilever-type inertial sensor is depicted by the following formulae[11]. Sensitivity, S of a sensor is

$$S = K\frac{M_{pm}tL_b(1+f)}{2EI_z} \quad (1)$$

First resonant frequency, ω of a cantilever beam is given by an approximate explicit formula[9.11]

$$\omega = \sqrt{\frac{EI_z}{M_{pm}L_b^3}}\sqrt{\frac{6f^2+6f+2}{8f^4+14f^3+10.5f^2+4f+2/3}} \quad (2)$$

It is clear from Eqns (1) and (2) that for chosen dimensions of inertial sensor, increasing the mass of proof-mass (M_{pm}) increases the sensitivity at the cost of resonant frequency. Since both the factors are governed by contradictory requirements, optimisation can be obtained through maximisation of the product of the two i.e. sensitivity and bandwidth. This product would give the measure of performance of a sensor[10]. This product is defined as *P*-factor.

3. MECHANICAL AND MODAL ANALYSIS OF CANTILEVER STRUCTURE

Simulations were run for fixed dimensions of flexure but for various lengths of proof-mass such as 800 µm, 1200 µm, 1600 µm, 2000 µm, and 3000 µm. The results of variation in stress on flexure and resonant frequency of these structures are plotted in Fig. 3. It is observed from the Figure that, when the proof-mass length is doubled (say from 800 µm to 1600 µm), the stress (sensitivity) increases by a factor of almost three-times but caused a reduction in resonant frequency by a factor of 2.5 times. The *P*-factor (i.e., sensitivity-bandwidth product) is found to have increased by a factor of 42 per cent but at the cost of large reduction in bandwidth, which may not be desirable. The values obtained through simulations were compared with analytical computations using Eqns (1) and (2). These were found in good agreement (within 10 % variation). It means that values from theoretical computation had deviation less than 10 per cent from FEM computations.

To increase sensor sensitivity, the other way is to increase the mass of proof-mass by way of depositing a planar layer of heavier material, all throughout the length of the proof-mass. Simulations were carried out for dynamic analysis of structure with fixed length and width of proof-mass, but by varying thickness of planar deposition from 6 µm to 26 µm of copper on the proof-mass. The results are shown in Fig. 4 that show variation in stress and frequency for different thicknesses of copper layer on the proof-mass.

It was observed from the simulation that when the mass of the proof-mass was doubled in this manner, the stress increases by a factor of 33 per cent whereas the frequency decreases by a factor

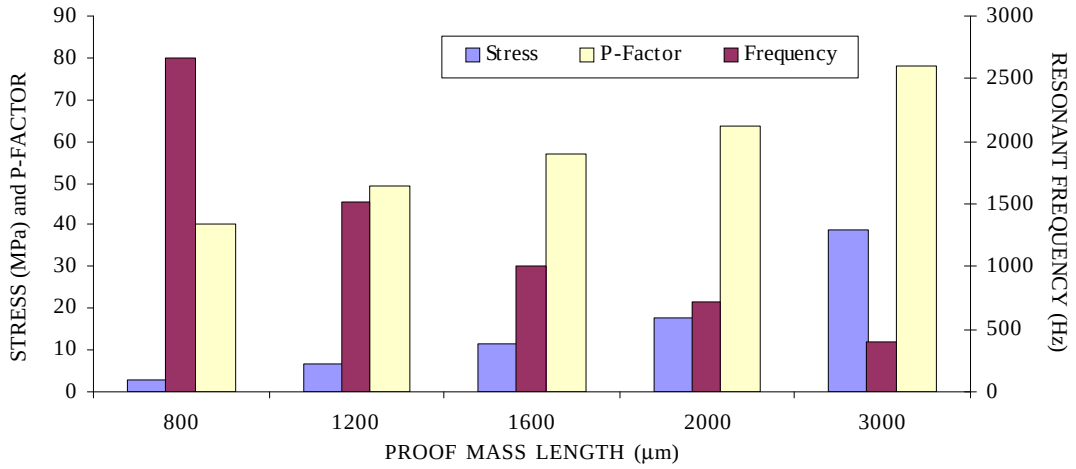

Figure 3. Variation in stress, *P*-factor and resonant frequency corresponding to proof-mass length.

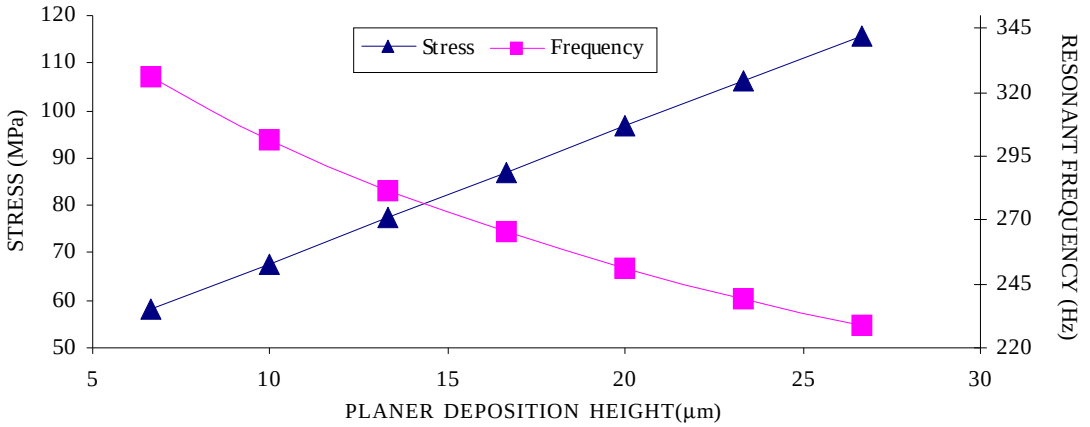

Figure 4. Variation in stress and resonant frequency corresponding to planar depositions on proof-mass for various deposition levels.

of 13 per cent, and the performance factor increases by a factor 15 per cent.

Deposition of planar copper layer on the proof-mass increases only the mass of proof-mass. Therefore the CG dependant factor *f* remains unaffected, as the CG of the structure is not changed. It is therefore thought of adding a lumped concentrated mass on the proof-mass. This modifies the CG of the structure and in turn modifies the factor *f*.

4. STRESS AND MODAL ANALYSIS OF CANTILEVER STRUCTURE WITH ADDED MASS

A structure is modelled which consists of a proof-mass having dimensions 3000 x 400 x 50 μm^3 (*l* x *b* x *t*), attached to a flexure of dimensions 100 x 8 x 50 μm^3 (*l* x *b* x *t*). An add-mass of copper having dimensions 400 x 400 x 100 μm^3 (*l* x *b* x *t*) is placed on the proof-mass at a particular distance from the fixed-end. Copper was chosen for its high density so as to magnify the variation in stress values with its position from the fixed-end. Figure 1 shows the geometry of the structure deposited with a lumped mass. This arrangement almost doubles the original mass of the structure.

Simulations were carried out by placing the add-mass at various locations from fixed-end to free-end along the longitudinal axis of the proof-mass. The advantage of using lumped mass is that, the CG of the structure goes on changing with each new position of the add-mass without any further addition of mass to the structure. This results in improvement of the *P*-factor of the structure. Figure 5 shows the variation in stress and frequency wrt position of add-mass along the longitudinal axis. The analysis of this graph depicts that the position of add-mass determines the sensitivity and resonant frequency of the structure, which in turn determines *P*-factor for the structure. In Fig. 5 for the add-mass positions, say at 500 µm from the fixed-end and at 2200 µm from the fixed-end, it can be seen that *P*-Factor increases by a margin of 20 per cent, Stress increases by a factor of 44 per cent whereas resonant frequency reduces by a factor of 30 per cent only.

Results of structure with planar deposition are compared with that of structure with add-mass in Fig. 6. This Figure is a composite graph, which plots the frequency versus stress obtained by varying: (a) thickness of planar deposition and (b) add-mass position along the longitudinal axis. It is observed that better sensitivity was achieved for a chosen design bandwidth (above 250 Hz) in case of structure with add-mass. For example, if a sensor is to be designed for a particular bandwidth, say 300 Hz, the stress value that one gets for planar deposition of 10 µm, is 67 MPa, whereas in the case of add-mass placed at about 1500 µm from the fixed-end for the same bandwidth, one gets a much higher stress value, of the order of 79 MPa. This indicates that one gets better sensitivity-bandwidth product for the structure with add-mass compared to the structure with planar deposition.

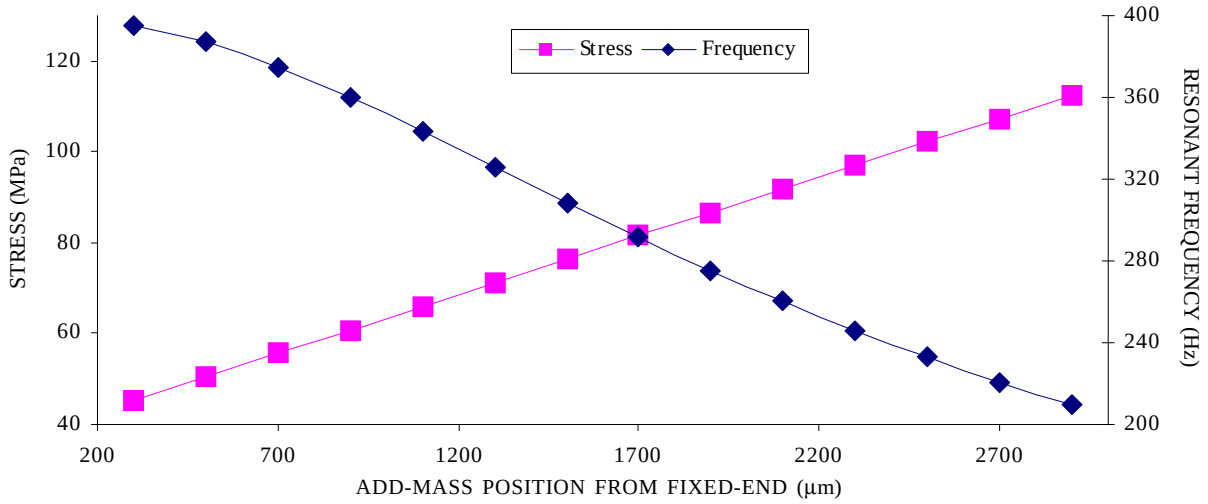

Figure 5. Variation in stress and resonant frequency corresponding position of add-mass on the proof-mass from fixed-end.

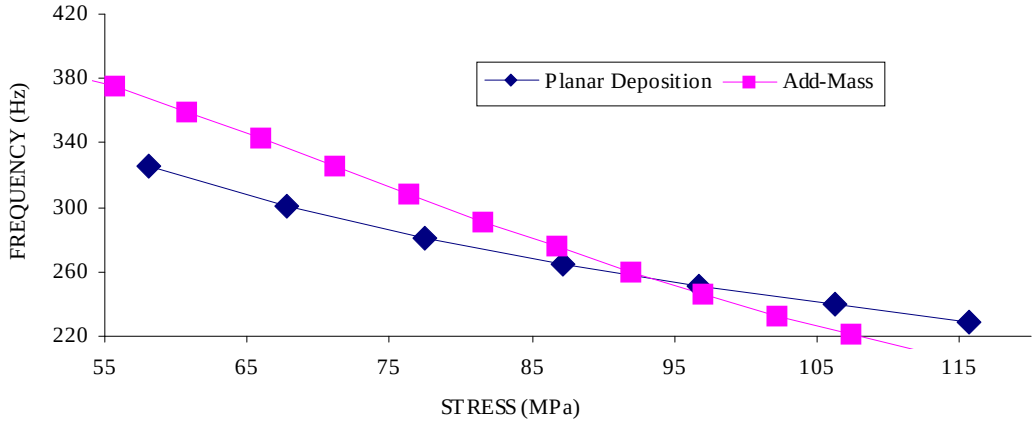

Figure 6. Performance comparison between planar deposited and add-mass structures.

5. MECHANICS OF CANTILEVER WITH ADD-MASS

The mechanics behind the peculiar behaviour of cantilever with add-mass can be explained using Euler's bending moment theory[15]. Figure 7 shows the schematic representation of cantilever beam. When the inertial force is applied to such a cantilever along *Y*-axis, it develops moment about fixed-end, which is directly proportional to CG of the structure for the applied force. Therefore, when the add-mass is moved from the fixed-end, the CG of the structure also moves away from fixed-end of the structure, and hence, the moment increases. Assuming proof-mass to be stiffer than the flexure and a beam (flexure) having deflection *v*, modulus of elasticity *E* and moment of inertia I_z about *Z*-axis, force *F* acting at a distance *C* from the fixed-end, the bending moment, *M* for a force acting at any location *X* from the fixed end is given[8,15] by following relation:

$$EI_z v'' = M = -F(C - X) \tag{3}$$

Integrating Eqn (3) twice and applying boundary conditions such that at $X = 0$, $v` = 0$, and at $X = 0$, $v = 0$, one gets a relation for beam deflection

$$EI_z v = -F\left(\frac{C.X^2}{2} - \frac{X^3}{6}\right) \tag{4}$$

$$v = -\frac{F}{EI_z}\left(\frac{C.X^2}{2} - \frac{X^3}{6}\right) \tag{5}$$

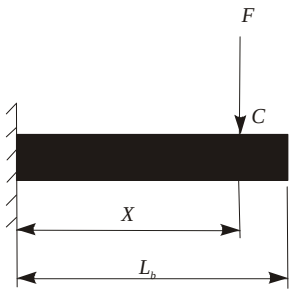

Figure 7. Schematic of cantilever beam.

Therefore, as CG shifts, the flexure deflection increases for the same value of applied force, and hence, the stress developed increases. However, frequency of a structure is a function of flexure stiffness k and mass M_{pm} of the attached proof-mass.

$$\omega = \sqrt{k / M_{pm}} \tag{6}$$

Where, k = force/deflection = F/v. Frequency of a structure is inversely proportional to the square root of flexure deflection, and in turn to the CG of the structure. Therefore for a flexure of length L_b, its deflection is given by

$$v = -\frac{F}{EI_z}\left(\frac{C.L_b^{\,2}}{2} - \frac{L_b^{\,3}}{6}\right) \tag{7}$$

Substituting for k and v, one gets

$$\omega = \sqrt{\frac{F}{v.M_{pm}}} = \sqrt{\frac{E.I_z}{(c.L_b^{\,2}/2 - L_b^{\,3}/6).M_{pm}}} \tag{8}$$

Therefore, as seen from Eqns (1) and (5), when add-mass is moved from fixed-end toward the free-end, the CG of the structure moves towards the free-end, and hence, stress developed in the flexure increases linearly. However frequency of the structure decreases nonlinearly [Eqns (2) and (8)]. Therefore, the sensitivity-bandwidth product for various positions of add-mass has a nonlinear behaviour. This analytical model supports the results obtained from simulations as discussed in Section 4.

6. SENSOR'S PERFORMANCE FACTOR MAXIMISATION THROUGH ADD-MASS POSITION SELECTION

Figure 8 shows plot of *P*-factor versus various add-mass positions for various proof-mass lengths, from 1400 μm to 3000 μm. A peculiarity can be observed that the curve shows a maximum at one particular position of add-mass. This indicates the optimum position of add-mass for the maximum *P*-factor. To locate the exact optimisation point, simulations were carried out for various positions of add-mass with fine stepping along *X*-axis nearer

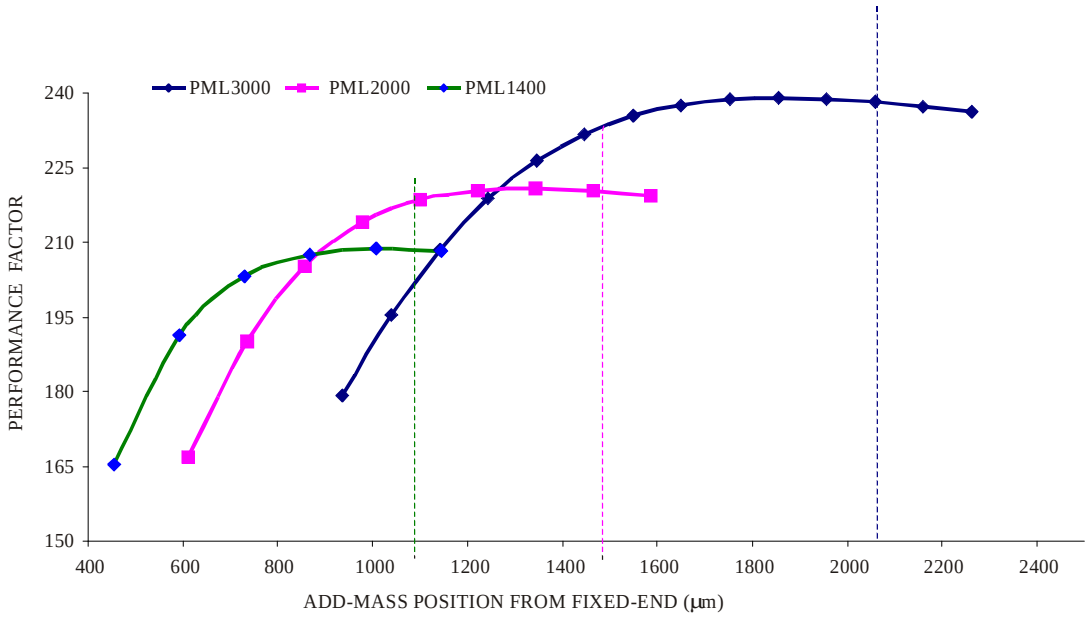

Figure 8. Variation in *P*-factor corresponding to add-mass position along proof-mass.

to the expected maximum of *P*-factor. The simulations were repeated for three lengths, viz., 1400 m, 2000 m and 3000 m. It was observed that the *P*-factor maximises for add-mass location of about three-fourth length of proof-mass. At this location of add-mass, the CG of the structure is found to be located at exactly two-third length of the proof-mass. It can therefore be inferred that to achieve optimised *P*-factor, add-mass should be positioned on the proof-mass to adjust CG of the overall structure at two-third length of proof-mass.

Another advantage of add-mass technique for cantilever-type inertial sensors is in choosing the two important sensor parameters, i.e., sensitivity and bandwidth. The different positions of add-mass from the fixed end on the proof-mass give different sensitivity and different bandwidth for the sensor. One gets higher sensitivity by placing add-mass towards the free-end, whereas one gets higher bandwidth for add-mass located near the fixed-end. By fixing one of the parameters, say sensitivity, one can place the add-mass at a particular location from the fixed end on the proof-mass to get maximum bandwidth for the sensor or vice versa.

7. DISCUSSIONS AND CONCLUSIONS

Investigations on the design optimisation for piezoresistive acceleration sensor in respect of optimisation of sensitivity and bandwidth has been the issue of research for a long time and will still continue to be so. Till now the focus of inertial sensor design was concentrated only on spring-mass system (i.e. involving flexure and proof-mass). Here, a new concept of add-mass on proof-mass has been introduced for cantilever-type of accelerometer and the structure is analysed using CAD model to bring out its advantages for choosing the two most important parameters, i.e., sensitivity and bandwidth of piezoresistive type of inertial sensor design. This technique involves placing of a high-density concentrated mass on the proof-mass at a position to seek maximum *P*-factor.

A very peculiar result in respect of position of add-mass indicates that to maximise the performance of inertial sensor the add-mass should be positioned at three-fourth length of the proof-mass. This position of the add-mass gives the maximum *P*-factor i.e., maximum product of sensitivity and bandwidth, thus indicating the optimised performance. The simulations also indicate that the structure with add-mass gives better bandwidth as compared to planar deposition on proof-mass. It is therefore possible to control the two important design parameters of piezoresistive inertial sensor as per need. The deposition of planar thickness all throughout the proof-mass is practicable. However, deposition of lumped mass (add-mass) on the proof-mass is feasible by way of fabrication by methods of casting and LIGA techniques.

ACKNOWLEDGEMENTS

The authors thank the Director, Armament Research and Development Establishment, Pune, for funding the research work on the development of micro-accelerometer at the University of Pune. Shri B.P. Joshi, Scientist F, would like to thank the Director ARDE for giving him the opportunity to work on the project. Shri B.P. Joshi also conveys his heartfelt thanks to Dr S.K. Salwan, his Guide for PhD, for his precious guidance and Shri J.K. Bansal, Associate Director, for his support and suggestions.

REFERENCES

1. Plaza, J.A.; Esteve, J. & Lora-Tamayo, E. Simple technology for bulk accelerometer based on bond and etch-back silicon on insulator wafers. *Sensor Actuators*, 1992, **A68**, 199-302.

2. Plaza, J. A.; Esteve, J. & Cane, C. Twin-mass accelerometer optimisation to reduce the package stresses. *Sensors Actuators*, 2000, **A80**, 199-07.

3. Chen, H.; Bao, M.; Zhu, H. & Shen, S. A piezoresistive accelerometer with a novel vertical beam structure. *Sensors Actuators*, 1997, **A63**, 19-25.

4. Partridge, A.; Reynolds Kurth, J.; Chui, B.W.; Eugene & Chow, M. A high-performance planar piezoresistive accelerometer. *Journal MEMS*, 2000, **9**(1), 58-66.

5. Butefisch, S.; Schoft, A. & Buttgenbach, S. Three-axes monolithic silicon low-g accelerometer. *Journal MEMS*, 2000, **9**(4), 551-56.

6. Aikele, M.; Bauer, K.; Ficker, W.; Neubauer, F.; Prechtel, U.; Schalk, J. & Seidel, H. Resonant accelerometer with self-test. *Sensors Actuators*, 2001, **A90**, 161-67.

7. Plaza, J.A.; Collado, A.; Cabruja, E. & Esteve, J. Piezoresistive accelerometers for MCM package. *Journal MEMS*, 2002, **11**(6), 794-01.

8. Van Kampen, R.P. & Woffenbuttel, R.F. Modelling the mechanical behaviour of bulk-micro machined silicon accelerometers. *Sensors Actuators*, 1998, **A64**, 137-50.

9. Roylance, L.M.; & Angell, J.B. A batch fabricated silicon accelerometer. *IEEE Trans. Elect. Devices*, 1979, **ED-26**, 1911-917

10. Soloman, S. Sensors handbook. MGH Publications, 1998.

11. Seidel, H. & Csepregi, L. Design optimisation for cantilever-type accelerometers. *Sensors Actuators*, 1984, **A6**, 81-92.

12. Lim, M.K.; Du, H.; Su, C. & Jin, W.L. A micro machined piezoresistive accelerometer with high sensitivity: Design and modelling. *Microelectronic Engineering*, 1999, **49**, 263-72.

13. Mermertas, V. & Erol, H. Effect of mass attachment on the free vibration of cracked beam. *In* 8th International Congress on Sound and Vibration, July 2001, Hong Kong, China.

14. Madaou, M. Fundamentals of microfabrication. CRC Press, New York, 1997.

15. Gere, J.M. Mechanics of materials. Chapman & Hall, London, 2000.